

## Real World Evaluation of a New Environment Adaptive Localization System

Ashok-Kumar Chandra-Sekaran<sup>2</sup>, Peter Schenkel<sup>1</sup>, Christophe Kunze<sup>2</sup>, Klaus D. Müller-Glaser<sup>1</sup>  
*Institute for Information Processing Technology (ITIV), Karlsruhe Institute of Technology (KIT),  
Germany.* <sup>1</sup> FZI Research Centre for Information Technology, Karlsruhe,  
(chandra,kunze)@fzi.de, peter.schenkel@igs-solution.de, kmg@itiv.uka.de,

**Abstract**— In order to assist the responders during disaster management a self-organizing, scalable, heterogeneous and location aware WSN architecture called Disaster Aid Network (DAN) was proposed in our previous work. One of the main aspects of DAN is the localization aspect which deals with the development of a subsystem for patient localization at the disaster site. The patient localization is split into ranging and position estimation tasks. In this paper a new environment and mobility adaptive signal strength based ranging technique for range estimation is proposed and is tested using both close-to-reality simulations and empirical analysis. These range information is given as input to a particle filter based position estimation algorithm previously proposed by us to provide the location estimate of the patient. In this paper a new localization system is setup by implementing this ranging and position estimation technique in a ZigBee network. A real world evaluation of this localization system is undergone and its localization performance is analyzed.

**Keywords**- Emergency response; ZigBee; Ranging; position estimation; Localization system, Real world evaluation.

### 1. Introduction

In Wireless Sensor Networks (WSN) researchers are dealing with challenges like heterogeneous networks, scalability, self-organisation, self-sufficient operation, multi-hop communication, ad-hoc networks and localization. Some of the short range wireless communication standard based technologies that can be considered for WSN are Bluetooth, ZigBee [3], RFID, etc.

The potential problems faced in the aftermaths of a disaster are: response capabilities of the local jurisdiction may be insufficient, large-scale evacuations from the disaster site, complications in implementing evacuation management strategy, disruption of critical infrastructure, large number of casualties, long duration to obtain an initial common operating picture [23].

We proposed a new emergency response system based on the Disaster Aid Network (DAN) architecture

to improve emergency response at the disaster site in [2]. DAN is a self-organizing, scalable, heterogeneous sensor network (see figure 1) of 30-200 nodes comprising of:

- Patient nodes with electronic triage tag and optional continuous vital sign monitoring. They are also called blind nodes [16] because their positions are unknown and have to be estimated.
- Pseudo anchor nodes are patient nodes whose positions are already estimated.
- Doctor nodes (mobile anchor nodes) are mobile nodes (Tablet PC) whose locations are known.
- The monitor station is a collector node which collects the patients' locations and visualizes them for the organization chief.
- Static anchor nodes are nodes placed at fixed positions whose locations are already known.
- Server: A server running a database for data collection and aggregation is placed at the management centre.

Based on the functionalities and operational setup, the design and development of DAN system can be classified into four aspects as follows: communication, localization, data aggregation and visualization, and sensor-actuator. This paper focuses on the localization aspect of DAN which is critical for the DAN system.

### 2. DAN Localization Aspect

The localization aspect deals with the development of a subsystem for localization of patients at the disaster site. Each patient node localizes itself on the occurrence of an event and communicates its location along with other relevant patient information to the server. The monitor station runs a visualization software that receives a patient's location from the database of the server and displays it on a disaster sitemap. The real time patient location information among others has two main use cases.

- The responders can track each patient in real time. This avoids the time consuming search

for missing patients at the site (ex: minor injury patients can run away from the site without informing the responders)

- The patient location helps to provide the responders with the number of patients belonging to each disaster site zone and patient flow rate between these zones leading to efficient resource (distribution of doctors, ambulances, etc.) planning.

This can improve situation awareness of the responders and assist in efficient resource planning and distribution. The organization of supply and service or logistics can be improved and the patients' do not need to wait before being evacuated to the hospitals.

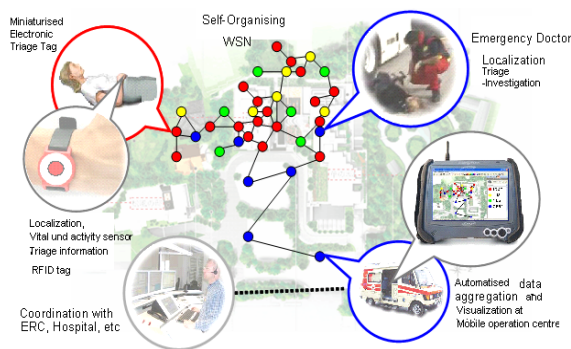


**Fig. 1. DAN System**

In this paper, the specifications for the localization aspect are formulated and a patient localization methodology is proposed. A new environment and mobility adaptive ranging technique (to estimate the distance between a blind node and its neighbouring nodes) that suits our localization specification is developed and analyzed using both simulation and empirical analysis. This distance information is given to the position estimation algorithm of the patient node which estimates the actual location of the patient in two dimensions. A new position estimation technique that is already developed and tested via close-to-reality simulations is briefed in this paper. Furthermore, these range and position estimation techniques are implemented and its real world evaluation in an outdoor environment is performed.

## 2.1 Patient Localization Specification

The specifications for patient localization at the disaster site are: handle the different environments (both outdoor and indoor); use minimum or no special infrastructure (static anchor nodes) due to lack of deployment time; track 30-200 patient nodes moving

with varying speed (0 to 3 m/s); attain an accuracy of around 10m; be scalable and robust. Even though accuracy is important the main challenge here is to handle the varying mobility and different environment with adverse RF conditions and also use minimum or no infrastructure.

## 2.2 Patient Localization Methodology

At the beginning of the emergency response, the portable monitor station (typically a notebook is setup. The static reference nodes are deployed manually in such a way that the network coverage is provided to the entire disaster site. Each emergency doctor is typically equipped with a doctor node which acts as mobile reference node. Once a patient is found, the doctor provides a wearable patient node, which is a blind node in terms of localization and needs to be localized over time. Therefore each patient node runs a decentralized localization algorithm. The patient localization methodology is divided into two parts called ranging and position estimation. Each part is addressed separately before combining them to yield the final patient location estimate. The ranging part estimates the distance (range) between the blind node (node whose location has to be estimated) to its neighboring reference nodes (nodes whose locations are already known). These range estimates are input to a position estimation algorithm running on the blind node which provides two dimensional real time location estimations of the blind node (patient).

### 2.2.1 Ranging Methodology

Range free techniques perform well when reference nodes are deployed uniformly throughout the site. As the nodes are deployed randomly and move randomly at the disaster site, range-based technique can be expected to offer a better accuracy compared to its range-free alternative [21]. In the range-based technique we selected RSSI based ranging technique as it needs less infrastructure compared to its counterparts like TOA (Time of Arrival), TDOA (Time Difference of Arrival) or Angle-of-arrival. Since offline (finger printing) based RSSI ranging techniques are time consuming, needs prior knowledge of the deployment site and repetition of finger printing for minor environmental changes, we use an online based RSSI ranging technique. Comparing with other signal sources (Infrared, ultrasound, etc) a radio frequency (RF) signal source is preferable because it is cost effective and provides a suitable transmission range indoor and outdoor. Therefore, we have selected an online RSSI-based ranging technique using the RF signal for distance estimation during patient localization [1].

Having selected an RSSI range-based technique for the distance estimation, a SOA analysis of RSSI based ranging algorithms has to be done. A new ranging technique for the patient localization has to be developed. A real world offline ranging database has to be built and given as input to the simulation model of the new ranging technique to obtain the distance estimates and their ranging performance has to be analyzed. The ranging technique developed has to be improved to exceed the limitations of the first stage of development.

### 2.2.2 Position Estimation Methodology

The ranging methodology proposed in the previous section will provide the distance estimates to the position estimation part whose methodology is explained in this section.

The DAN system consists of anchor and patient nodes that are either static or mobile. The patient nodes can move (actively or passive) in an undefined manner (patients moving from one zone to another, patients running away from site, etc.) or be static (red or yellow triaged patients lying down, etc.). Thus, DAN is seen as a dynamic and mobile WSN whose topology changes during its operation time. Mobility makes a WSN delay intolerant i.e. information gathering and localization is done in real time, depending on the speed of the nodes [6]. Besides, a localization algorithm for mobile WSN should cope up with temporary loss of anchors. So position estimates based on simple techniques (ex: trilateration) is unsuitable for our scenario. Mobility should be directly taken into account when designing localization algorithms for mobile WSN and Monte Carlo Localization (particle filter) based algorithms are suitable [6].

Our new system to localize patients at the disaster site can be characterised as a non linear and non Gaussian system with multimodal densities. Linear filters might even give good results for nonlinear, non-Gaussian systems if the system can be approximated by a linear, Gaussian system but in general nonlinear filter techniques are required. A particle filter approximates the posterior with a finite set of samples drawn from the posterior thereby allowing the representation of a broad class of densities including multimodal distributions. In general, a particle filter has superior accuracy over the EKF (Extended Kalman Filter) and the UKF (Unscented Kalman Filter) but this comes at the cost of higher computational effort. Due to the above stated reasons a particle filter based solution is chosen for our position estimation. A new particle filter based patient position estimation algorithm that suits our localization specification has already been developed by us and its performance is

analyzed using close-to-reality simulations [22]. In this paper this algorithm will be briefed.

The ranging and position estimation techniques have to be implemented in a ZigBee network and real world evaluated in an outdoor environment. This demonstrator is considered as a first release of the patient localization sub system for DAN.

## 3. State of the Art Analysis of Localization in WSN

The state of the art (SOA) localization system and RSSI based ranging algorithms related to our work are analyzed in this section

### 3.1 Localization Systems

Systems like Active Badge [8], Cricket [9], RADAR [10] required a lot of infrastructure. GPS [11] is not suitable for Indoor. In order to obtain a good GPS accuracy the following conditions have to be satisfied: proximity of GPS to buildings should be greater than 3 meters, device should not be brought under dense trees, antenna should be held firmly above shoulder height (approximately 2 meter), and point to the open sky. It is impossible to follow the conditions mentioned above for localizing patients at a disaster site which is an unknown environment with adverse RF conditions. RFID based solutions like SpotON [20] are not suitable for us since they demand high anchor node density, works in short range and needs a fixed infrastructure. We did a primitive analysis of the CC2431 localization solution [13, 4] from Texas Instruments (TI) and it revealed that the blind node location estimation is unstable and needs large number of reference nodes for considerable performance. So this system is also not suitable for our scenario. Therefore we started developing a new localization solution for our scenario.

### 3.2 RSSI Range-based Techniques

The works in [15], [17], [18], [19] discuss about RSSI based ranging techniques. It is difficult to compare the results of different SOA works due to different preconditions and lack of generally agreed test beds and testing protocols for such networks being available yet. Besides most of the SOA results have been obtained via simulation and real life evaluation are rarely used. We therefore limit the analysis in this subsection only to those algorithms that might have usability for our patient localization.

In [7], Kamin Whitehouse et. al. mentions that RSSI localization in unknown or changing environments needs to adjust system parameters such as signal strength and calibration coefficients automatically. In

[12] Erin-Ee-Lin Lau et. al. proposes a centralized ranging technique using RSSI smoothing and a position estimation technique. The CC2431 ranging technique [13] from CC2431 localization solution (from Texas Instruments) estimates the range between a blind node and a reference node by measuring the average RSSI value between them which is used directly for the distance estimation.

#### 4. New Ranging Technique

In this section a new method named Ranging using Environment and Mobility Adaptive RSSI method (REMA) for patient localization during disaster management is proposed [1]. Based on the simulation results of REMA this technique is further improved to propose “Improved REMA” technique. The localization specifications (see section 2.1) imply that the blind node movement is arbitrary, blind node velocity changes over time, the environment conditions change over time, and an approximate node density of around 300 m<sup>2</sup> /reference node.

##### 4.1 Ranging using Environment and Mobility Adaptive RSSI method (REMA)

To combat both the static and mobile variations of RSSI during range measurements effectively, we propose REMA which divides the problem space into two and address them separately before combining them to yield the final distance estimation.

- Static variations compensation: by applying online path loss estimation
- Mobile variations compensation: by applying smoothing algorithm on the static variations compensated distance

The key takeaways from SOA algorithms that act as a base for REMA are as follows. We have used the smoothing algorithm from Erin-Ee-Lin Lau et. al. [12] as an initial step. From our experiments and the experimental results of Kamin Whitehouse et. al. [7] we have understood the need for calibration of path loss coefficients to reflect environmental changes. Along with these key takeaways, we have introduced the following main new features in the REMA:

- A range estimation concept that combines calibration of path loss coefficient technique and distance (or range) smoothing.
- Online path loss estimation: The path loss coefficient estimation is carried out throughout the life of the network, to closely track the

environment changes around the reference node. The existing reference node setup is used to estimate the path loss coefficient for each reference node.

- An offline RSSI database built through indoor and outdoor real world experimentations is used to analyze the algorithm’s performance.

Each blind node runs the REMA for estimating its distance to each of its one hop anchor nodes. This estimated distance is fed as input to a position estimation algorithm running on the same blind node. Figure 2 shows the steps carried out in REMA method which are explained as follows.

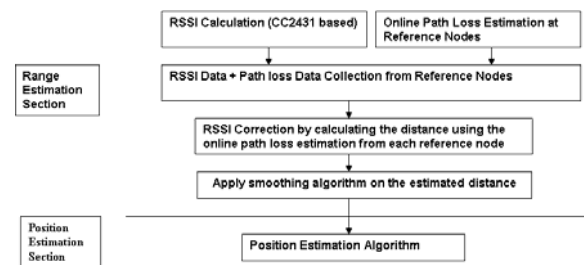


Fig. 2. REMA Flow Diagram

##### 4.1.1 RSSI Calculation

Each blind node broadcasts a burst of packets to its one hop reference nodes and requests the reference nodes to compute the average RSSI value. When the reference node receives a packet it will automatically add an RSSI value to the received packet. The RSSI value is always averaged over the 8 first symbol periods (128 μs) [13]. The reference node computes the average RSSI value by simply averaging the RSSI of all the received burst of packets (from the blind node). In addition to the RSSI value, each reference node is also requested to send its latest online path loss coefficient value estimated at that point of time.

##### 4.1.2 Online Pathloss Estimation

Using a single offline static path loss coefficient for all the reference nodes during range estimation does not reflect the changes in environment over time. So we propose an online position estimation technique where each reference node calculates the path loss coefficients online and periodically updates them. Now, each reference node repeats this pathloss estimation procedure in a time interval of say ‘Tn’ time units. A low value of ‘Tn’ results in more accurate distance estimation, for the cases of varying environment conditions. On the other hand, a low

value of ‘Tn’ slightly increases the communication overhead. So a trade-off between the reference node communication overhead (battery lifetime and available communication bandwidth) and distance estimation accuracy has to be achieved. When the path loss coefficients of all such reference nodes are combined over a given period of time, it represents the online path loss modelling of the entire environment (disaster site). Hence, our path loss estimation can be visualized as a discrete online path loss modelling. We consider it to be environment adaptive as it quickly updates the path loss model for the environment changes.

We propose an online path loss estimation technique called ‘averaging path loss’ for REMA. A reference node *i* broadcasts a burst of packets to its one hop reference nodes. A one hop reference node *j* computes the average RSSI value ( $avg.RSSI_{ij}$ ), and the pathloss coefficient  $n_{ij}$  between the reference node *i* and its one hop neighbour *j*. The  $n_{ij}$  is calculated by substituting the actual distance ( $d_{ij}$ ),  $avg.RSSI_{ij}$ , and the RSSI at one meter distance from a reference node (*A*) in equation 1. Similarly the pathloss coefficients between *i* and all its one hop reference nodes are calculated and averaged (periodically) to obtain the averaged path loss coefficient  $n_i$  that reflects the environment around *i*.

$$n_{ij} = \left( \frac{avg.RSSI_{ij} - A}{10 \log_{10} d_{ij}} \right) \quad (1)$$

#### 4.1.3 RSSI Correction

RSSI correction is a two step process which transforms the RSSI into a estimated distance between a reference node and a blind node. These steps are as follows:

Step I: The blind node requests and collects the RSSI and averaged path loss co-efficient *n* from each of its one-hop reference nodes.

Step II: The blind node computes its distance estimate  $d_{est}$  to each of its one-hop reference node using equation 2.

$$d_{est} = 10^{((RSSI - A) / (10 \times n))} \quad (2)$$

#### 4.1.4 Smoothing Filter

After RSSI correction phase, the smoothing filter of Erin-Ee-Lin Lau et. al. is adapted for our scenario and applied on the estimated distance to get the final smoothed distance. These point to point distance

estimation values are fed as input to the position estimation algorithm. This distance smoothing algorithm assumes:

- The blind node does not move arbitrarily in the test bed
- The blind node moves with a constant velocity

The distance (range) smoothing algorithm is a four step process as explained below:

Step 1: The estimated range for the  $i^{th}$  update is given by equation 3.

$$\hat{R}_{est(i)} = \hat{R}_{pred(i)} + a(R_{prev(i)} - \hat{R}_{pred(i)}) \quad (3)$$

Where,  $\hat{R}_{est(i)}$  = the *i*th smoothed estimate range,

$\hat{R}_{pred(i)}$  = the *i*th predicted range,

$R_{prev(i)}$  = the *i*th measured range,

The filter constant ‘a’ attenuates the large deviations or ignores the large deviations between the measured and predicted range values.

Step 2: The estimated range rate for the  $i^{th}$  update is given by equation 4 where, *b* is a filter constant. Range rate estimation works identical to the range estimation explained in Step 1.

$$\hat{V}_{est(i)} = \hat{V}_{pred(i)} + \frac{b}{T_s}(R_{prev(i)} - \hat{R}_{pred(i)}) \quad (4)$$

Where,  $\hat{V}_{est(i)}$  = the *i*th smoothed estimate range rate,

$\hat{V}_{pred(i)}$  = the *i*th predicted range rate,

$T_s$  = time segment upon the  $i^{th}$  update.

Step 3: The predicted range  $\hat{R}_{pred(i+1)}$  for the  $i+1^{th}$  update is given by the equation 5.

$$\hat{R}_{pred(i+1)} = \hat{R}_{est(i)} + \hat{V}_{est(i)} T_s \quad (5)$$

Step 4: The predicted range rate  $\hat{V}_{pred(i+1)}$  for the  $i+1^{th}$  update is given by the equation 6.

$$\hat{V}_{pred(i+1)} = \hat{V}_{est(i)} \quad (6)$$

One of the main limitations in this smoothing filter is the selection of filter gain constants ‘a’ and ‘b’. The filter gain constants are configured as  $a = 0.0625$  and  $b = 0.0625$  for both indoor and outdoor environments by performing offline data analysis using a sample dataset.

## 4.2 REMA Ranging Simulation

The REMA model that uses ‘averaging path loss’ technique for online path loss estimation and Erin’s smoothing filter for distance smoothing is simulated (via Matlab) in an outdoor and indoor test bed ranging database and the results are presented in this section. For simplicity the ‘average path loss’ technique estimates the path loss coefficient for each reference node only at the beginning of the data collection in the test beds i.e. a one time static path loss value is estimated for each reference node individually. The simulation results of REMA are compared with that of the SOA range estimation technique ‘CC2431-Ranging’ (see section 3.2). The ‘CC2431-Ranging’ uses a single static offline path loss value for all reference nodes which is selected as 3.25 (optimal) empirically.

### 4.2.1 Offline Ranging Database

This subsection explains the formation of a metadata based offline database by collecting ranging data at outdoor and indoor NLOS test beds. A ZigBee-compliant TI CC2430 node (see [5]) is used either as static reference nodes elevated at 1.5m height or a single mobile RSSI collector node. Reference localization systems are used to capture the actual path traced by a single mobile RSSI-collector node during experimentation. A test person carries a reference localization system and a single collector node and walks around (approximately 1m/s) in the test bed. At any time during our experiment duration of 50 minutes, the actual position of the collector node (from the reference localization system) and the RSSI from the static reference nodes are collected to form the ranging database.

Outdoor test bed: A 100x25m (approximately) outdoor parking space (see google image of outdoor test bed in figure 3) is setup with 8 reference nodes dispersed by 25m NLOS. The test bed comprises of static or mobile obstacles like people, cars, bikes, tree, trucks, bicycles, metal containers and rods. A differential GPS device acts as a reference localization system and is benchmarked at the test bed to obtain an average accuracy error of less than 2m.

Indoor test bed: A 23m x 12m (approximately) indoor area covering seven rooms and a corridor in the second floor of an office building (see figure 4) is setup with 7 reference nodes (one node in each room). The test bed comprises of static or mobile obstacles like people, computers, coffee machines, printers, walls, etc. The CC2431 location engine solution from TI [4,13] acts as a reference localization system (due to its availability with us, though not an optimal reference system) and is benchmarked at the test bed to obtain an

average error of 3.1m, maximum error value of 4.8m and minimum error value of 1.5m.

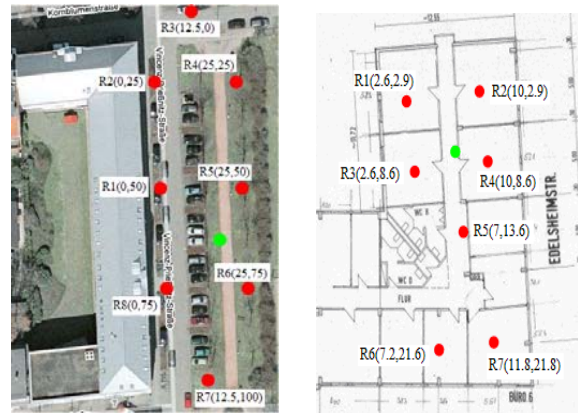


Fig. 3. Outdoor test bed Fig. 4. Indoor test bed

### 4.2.2 Results using Outdoor Database

The average ranging error (in terms of % of error in distance estimations) obtained using ‘CC2431-ranging’ and REMA method, during the distance estimation over time between the mobile node and each of the reference nodes R1 to R4, are as follows:

- R1, ‘CC2431-ranging’: 59.80% and REMA filter: 21.81%
- R2, ‘CC2431-ranging’: 80.05% and REMA filter: 42.04%
- R3, ‘CC2431-ranging’: 85.93% and REMA filter: 38.18%
- R4, ‘CC2431-ranging’: 74.39% and REMA filter: 38.69%

In all above cases (R1 to R4) REMA outperforms ‘CC2431-ranging’ in the outdoor environment.

Figure 5 plots the frequency distribution of distance estimation error in outdoor environment of all reference nodes combined together over the error intervals (in meters). Comparing the frequency distribution of error of CC2431 ranging and REMA filter, it is found that the REMA filter shows high probability of getting low error values and low probability of getting high error values. This indicates that the distance estimation of REMA filter is more accurate than that of the CC2431 ranging in the outdoor environment.

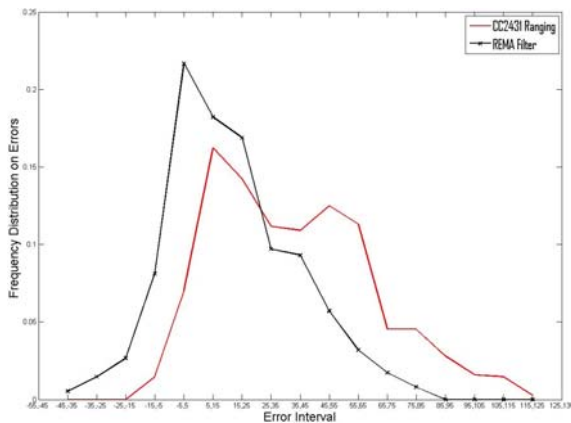


**Fig. 5. Frequency distribution of error**

#### 4.2.3 Results using Indoor Database

The average ranging error (in %) obtained using ‘CC2431-ranging’ and REMA, during the distance estimation between the mobile node and each of the reference nodes R4 to R7, are as follows:

- With respect to R5, ‘CC243-ranging’: 73.5% and REMA filter: 40.89%
- R4, ‘CC243-ranging’: 59.05% and REMA filter: 40.89%
- R6, ‘CC2431-ranging’: 65.05% and REMA filter: 36.84%
- R7, ‘CC2431-ranging’: 82.30% and REMA filter: 66.84%

In the above cases (R4 to R7) REMA filter outperforms ‘CC2431-ranging’ in the indoor environment as well. The distance estimation error for indoor setup is worse than that of the outdoor approximately by a factor of two.

#### 4.2.4 Summary

The REMA ranging method (with ‘averaging path loss’ and Lau et. Al. smoothing algorithm) is simulated using an offline ranging database and the results are that REMA reduces the overall average range estimation error by about 31% when compared to the SOA ‘CC2431-ranging’ [1]. The results indicate that RSSI based ranging is a feasible solution for the patient localization at least in outdoor environments even though considerable estimation errors at certain areas remain, while in indoor the performance is severely affected. The REMA method is a suitable base for patient localization even though further improvements have to be done towards achieving the targeted final accuracy.

### 4.3 Improved REMA Method

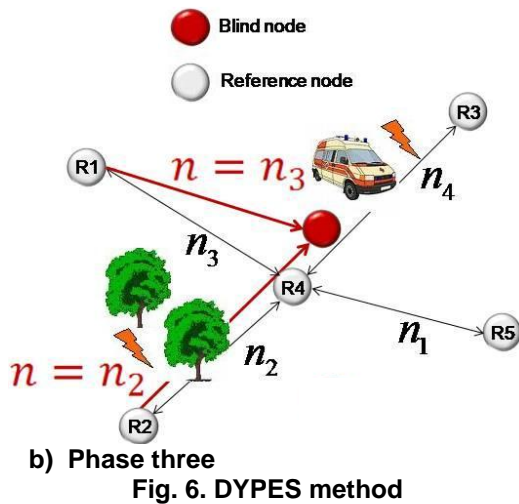
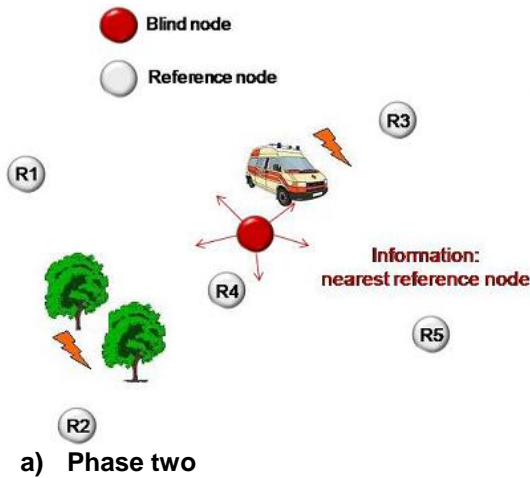
In this section the REMA method that uses ‘averaging path loss’ and Lau et. Al. smoothing algorithm is discussed and a concept to improve the online path loss estimation and smoothing filter is proposed leading to “Improved REMA”.

#### 4.3.1 Online Path loss Technique Improvement

The ‘averaging path loss’ technique proposed for online estimation in REMA method (see section 3.1.2) is only a simple approach. We have an exponential correlation between the path loss coefficient  $n$  and the distance  $d$  (see equation 1). So small changes in the path loss coefficient accounts for large changes in the distance. We therefore consider the accuracy of the path loss coefficient to be a critical issue for distance estimation and only a simple approximation by averaging is not sufficient for our purpose. So in this section we introduce a new online path loss estimation strategy to represent the real path loss value between blind node and reference node, which we call dynamic path loss estimation strategy (DYPES). The idea is to estimate an individual path loss for each blind node, depending on the area it is in. This strategy can be divided into 3 phases as follows:

- Each reference node collects signal strength and location from all other reference nodes with known location
- A blind node broadcasts the location of the reference node from which it receives the highest RSSI value (see Fig. 6 (a)), assuming that the distance is minimal.
- Each reference node sends an individual path loss to the blind node which is the path loss between itself and the reference node closest to the blind node (see Fig. 6 (b)).

Assuming the blind node is at the same position as a reference node the path loss calculation is optimal, the farer away from any reference node the worse the path loss estimation. We consider the accuracy of the path loss coefficient to be a function of the distance between blind node and nearest reference node. Figure 6 illustrates the new path loss estimation strategy.



### 4.3.2 Smoothing Filter Improvement

Erin Lau et. Al. smoothing algorithm is unsuitable with arbitrary movement, changes in directions and velocity of the blind node. Another critical issue is the parameter (filter gain constant) tuning as it is difficult to configure a generalized value that is versatile. Therefore in this section we check the three candidate filters to meet our requirements: handle arbitrary movement, handle different velocities, handle outliers and fluctuations of RSSI, and generalized parameters without further adaption. These three candidate filters are as follows:

- best-of-k filter, which uses the best obtained RSSI measurement from the previous k measurements as shown in figure 7.
- Erin’s smoothing algorithm as described in section 4.1.4

- combination of best-of-k and Erin’s smoothing filter

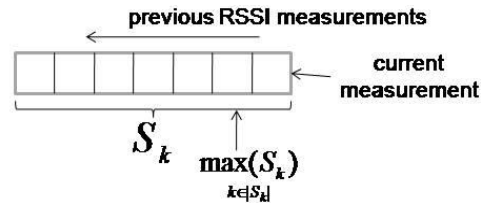


Fig. 7. Best-of-k filter scheme

We consider the best-of-k filter to be theoretically best-suited for our requirements as it attenuates fluctuations by ignoring up to k-1 outliers. We assume that a radio signal cannot be strengthened passively. Let  $\alpha$  be the upper bound for the received signal strength between 2 nodes, separated by a distance  $d$  and  $n$  be the path loss coefficient. Assuming a good estimation of  $n$  (an optimal estimation of  $n$  would naturally lead to the exact distance estimation if using  $\alpha$ ), the critical issue is to receive  $k$  RSSI measurements where at least one measurement is close to  $\alpha$ . The value of  $k$  is chosen such that it is large enough and doesn't impose too much delay to the system.

In the evaluation section, the three filters mentioned above will be evaluated using a real world RSSI database to select the best-suited filter. Even though distance smoothing is used in REMA, the Improved REMA (best-of-k and DYPES) uses RSSI smoothing. The method of Improved REMA is as shown in figure 8.

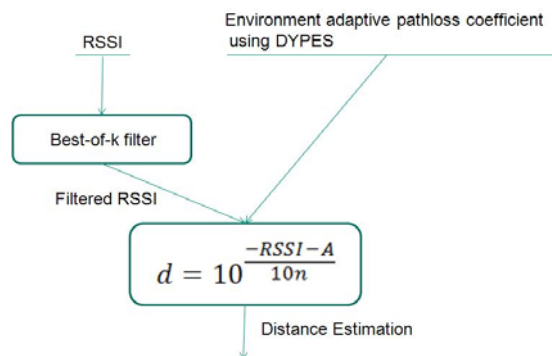


Fig. 8. Improved REMA method

## 5. Position Estimation Technique

In this section a new particle filter based position estimation algorithm for patient localization called Improved Range-Based Monte Carlo Patient Localization (IMPL) that was already proposed by us



in [22] is briefed. The distance estimates obtained by Improved REMA that works on a blind node is given as input to the IMPL which provides the patient position estimate. IMPL maintains a weighted sample set in order to estimate the patient node's position. IMPL undergoes three main steps: Prediction, weighting and resampling which are explained below.

**Prediction:** The prediction step depends on whether there's already an established sample set (after initialization) or not (during initialization).

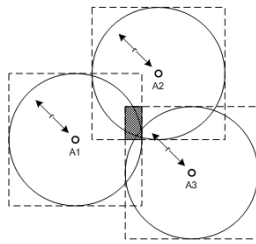


**Fig.9. Forming the anchor box**

In prediction during initialization, first the area to be sampled from is constrained to an anchor box. The region covered by the transmission range  $r$  of each one-hop anchor is approximated to a box as shown in figure 9. The overlapping area of all the boxes (shaded area in figure 9) forms the anchor box. Then a sample set of 40 uniformly distributed samples are drawn from the anchor box. In prediction after initialization, we take each sample from the previous time step and form a circle of radius  $v_{max} + addition$  centered at that sample's position. From every circle one new sample is drawn.

**Weighting:** A weight is calculated (based on the range measurements) for each sample in the sample set, to know if they are good or bad representations of the actual location of a blind node. In order to weigh a sample  $i$  of a blind node, all the range measurements of this blind node to its one-hop anchors are selected. Consider a range measurement  $rm_j$  between a blind node with a sample  $i$  and its one-hop neighbor  $j$ , then a partial weight  $wp_i^j$  is computed as shown in equation 7. Here the range measurement  $rm_j$  is projected onto a Gaussian distribution (see Fig. 10) of mean  $\mu = d + \mu_v$  (where  $d$  is the distance between the sample and the one-hop neighbor) and standard deviation  $\sigma_v$ . The  $\sigma_v$  and  $\mu_v$  of a Gaussian random variable  $v$  are the systematic and random error of the range measurement error model (of the environment).

Their values are deduced from the environment i.e. all anchor nodes within the transmission range of each other compute the error between their actual distance and their estimated distance. All these values are collected in a single node to calculate the  $\sigma_v$  and  $\mu_v$ .

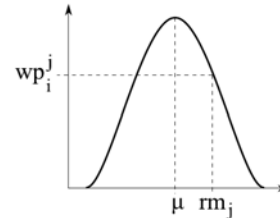


**Fig. 10. Calculating the partial weight**

The total weight  $w_i$  for sample  $i$  is the product of all partial weights.

$$wp_i^j = \left(1 / \sigma_v \sqrt{2\pi}\right) \cdot e^{-0.5(rm_j - \mu)^2 / \sigma_v^2} \quad (7)$$

**Resampling:** After normalizing the weights of the sample set to one, samples are redrawn from the normalized sample set with a probability proportional to their weights. The size of the new sample set remains the same.

The position estimate  $(x, y)$  of the blind node is calculated as the weighted mean of the sample set. The closeness value for blind node  $p$  with  $N$  samples is computed as in equation (7).

$$closeness_p = \sum_{i=1}^N w_i \sqrt{(x_i - x)^2 + (y_i - y)^2} / N \quad (8)$$

where  $(x_i, y_i)$  denotes the position of sample  $i$ ,  $w_i$  denotes the weight of the sample  $i$  and  $(x, y)$  is the current location estimate of node  $p$ . The closeness of an anchor node is set to 0.

IMPL has to be initialized with a set of parameters:

- Systematic and random error ( $\sigma_v$  and  $\mu_v$ ) of the range measurement error model.
- the transmission range  $r$  of the nodes
- the maximum velocity of the mobile node and additional factor which increases the circle to draw the samples ( $v_{max} + addition$ )
- the upper and lower bounds for the coordinate system

These parameters have to be found heuristically or can be set in an initialization phase automatically.

## 6. Real World Evaluation

In this section our new ranging and position estimation techniques for patient localization are implemented and the position estimation performance is evaluated in a realistic scenario. We compare the obtained results with a state-of-art localization system from Texas Instrument in section 7.

### 6.1 Test Bed

For evaluating our system we implement our ranging and position estimation algorithm on a ZigBee-ready hardware node of the CC2520ZDK development kit from TI. This ZigBee-ready node comprises of a MSP430F2618 16-bit ultra-low power micro controller connected to a 2.4 GHz IEEE 802.15.4 RF transceiver, SMA antenna. Each device is either used as reference node or blind node in our experiment. Each reference node is placed in a transparent plastic box mounted on a tripod at a height of 1.5m and are distributed on the experiment site. The SX2 Hemisphere DGPS is used as a reference. A person carries a DGPS mounted on top of a rucksack and also a single blind node mounted next to the DGPS antenna in a transparent plastic box and walks randomly in the experiment site. At any time during the experiment, the actual position of DGPS and the estimated position of the blind node are recorded. Accuracy error is plotted as Euclidean distance between the recorded DGPS position and the estimated position of our system.

We define two experimental test beds. A line-of-sight area (LOS) and a non-line-of sight area (NLOS). The LOS area is a football field of around 80m x 45m with a reference node density of around 450m<sup>2</sup>/node and is an obstacle free area with line of sight between all nodes as shown in the google image in Fig. 11. The NLOS area is around 60m x 30m with a reference node density of around 225m<sup>2</sup>/node. This area includes a parking lot and a walking pathway with trees. It has obstacles such as metal containers, cars, fences and trees as shown in the google image in Fig. 12. The black dots within the experiment area represent the positions of the localized reference nodes. All our experiments explained in this chapter are done in these test areas unless otherwise stated. In order to compare the data of LOS and NLOS areas, experiments are done with exactly the same setup and the data is recorded in the same session.

Since DGPS is used as reference system its accuracy is benchmarked at our experiment site and an average accuracy error of less than two metres is obtained. We therefore conclude that DGPS is a suitable reference system in this area. The reference node localization

and placement are topics of concern. In our experiment the reference nodes are localized using DGPS. The reference nodes are localized by first setting DGPS to zero on a certain reference node (origin) and programming the remaining reference nodes locations with respect to the origin. For each chosen reference node it is checked that the DGPS position does not fluctuate more than 2m by observing the DGPS position for 60 seconds at a specific position. The reference nodes are placed near the edges and within our experiment area, without any special placement strategy.



Fig. 11. LOS test bed with reference node positions

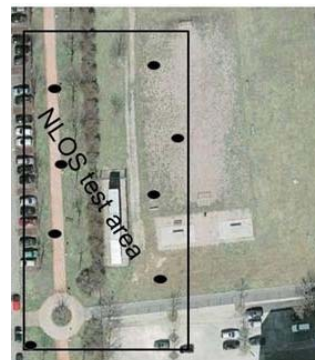


Fig. 12. NLOS test bed with reference node positions

### 6.2 Evaluation Results

In this section we present the results of different intermediate evaluation steps, leading to the testing of our final localization system in a NLOS test area. In the first subsection we test different RSSI smoothing filters in simulation to determine their performance. In the second subsection we test our ranging technique by combining a smoothing filter and DYPES. In the third subsection we test our position estimation performance.

### 6.2.1 RSSI Smoothing Filter

An RSSI database is given as input to a simulation model to test filters such as best-of-k, REMA using Erin's smoothing algorithm, 'REMA using Erin's smoothing algorithm and best-of-k combined' (see section 4.3.2). The ranging error is evaluated as Euclidean distance of the DGPS position to a reference node and the estimated distance.

#### Offline Outdoor RSSI Database

An offline database is collected by recording RSSI values each second with a blind node which moves randomly in the LOS test area as described in section 6.1 and figure 11). The data for each time step consists of the actual position of the blind node recorded by DGPS and accordingly the recorded RSSI value. In total the database consists of 10,251 such tuples divided into 8 subsets, each containing the collected data received from one reference node.

#### Simulation of RSSI Smoothing Filters

For determining the free filter parameter values (to be defined later in this section) we use a cross-validation with up to 5 randomly chosen subsets for training, and 3 randomly chosen subsets, excluding the training data, for evaluating the quality of an obtained set of filter parameters. An exhaustive search over possible values is performed.

This search also leads to an evaluation of the influence of these parameters as well as their robustness in a LOS environment. The values of the following parameters have to be estimated:

- A : the parameter which describes the signal strength at 1m distance (in dBm)
- k : the number of past RSSI values used for the best-of-k filter
- a : filter gain constants (distance) for Lau et. Al. smoothing algorithm
- b : filter gain constants (speed) for for Lau et. Al. smoothing algorithm
- path loss : the path loss coefficient suited best for the data obtained data

Figure 13 shows the mean ranging error of the three filters, obtained by varying the number of training sets used to estimate the parameters. With an increasing number of training sets the average range error decreases for each of the tested filters, as the parameter estimation is more general with each added set of data. However, at the right end of the plot, we see an increasing error for all filters except the best-of-k

filter. We consider this effect as a result of over fitting; the parameters have been adapted too much to the training set, such that its power to generalize to unseen data decreases. With an increasing number of estimated parameters, over fitting becomes a critical issue. The filter with the highest number of parameters ('REMA using Erin's smoothing algorithm and best-of-k combined': 5 parameters) performs significantly worse after reaching a certain amount of training data. REMA using Erin's smoothing algorithm (4 parameters) performs better, but as well we can see the same tendency. The best-of-k (3 parameters) is almost unaffected by the amount of training data.

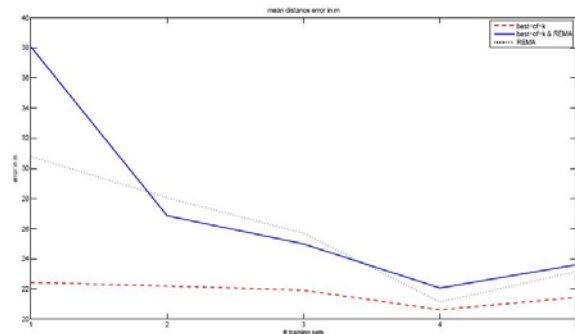


Fig. 13. Mean ranging error for different filters

#### Conclusion

Filters with a small number of free parameters need less time to converge and are more robust in terms of the amount of training data for LOS environments. Therefore we select the best-of-k filter for RSSI smoothing for Improved REMA Ranging.

### 6.2.2 Ranging using Improved REMA

We implement an Improved REMA that comprises a best-of-k filter for RSSI smoothing in the blind node and DYPES for online path loss estimation (see section 4.3.1) and evaluate its performance in our LOS and NLOS test area as described in section 6.1. The parameter 'A' should be determined by measurement but due to the fluctuating signal strength it cannot be defined clearly. We therefore use  $A = 48\text{dBm}$  as this showed best performance and  $k = 3$  for the best-of-k filter for all evaluations further on, as this is a good trade-off between latency of the system and for discarding outliers. The range and path loss is updated every second. However, we are aware of the fact that this setting comes along with a large amount of traffic in the network but consider it as a good benchmark setting to achieve maximum accuracy.

In the LOS test area the mean ranging error obtained is 12.21m, in the NLOS area the mean ranging error is 10.93m. We call the Improved REMA's performance

out-of-the-box as there is no parameter tuning necessary before deploying the system. Table 1 shows the results obtained in the ranging experiments. Against our expectations the ranging error in the NLOS area is smaller than in the LOS area. We believe that this is due to the deployment area for both experiments. The node coverage in the NLOS area is twice as high (225m<sup>2</sup>/reference node) compared to the LOS area (500m<sup>2</sup>/reference node).

Test area	Area	RN	Mean error
LOS	80m×45m	8	12.21m
NLOS	60m×30m	8	10.93m

**Table 1. Ranging performance summary**

**6.2.3 Localization using Improved REMA and IMPL**

We implement an Improved REMA consisting of a best-of-k filter for RSSI smoothing and DYPES for online path loss estimation. For position estimation we use IMPL (see section 5). The performance of the system is evaluated in our LOS and NLOS test area as described in section 6.1. The experiments as described in section 6.2.2 and 6.2.3 are done in the same session for each test area (LOS and NLOS) so that we can compare the ranging and position estimation error for similar environmental conditions. Figure 14 shows a complete scheme of the localization process.

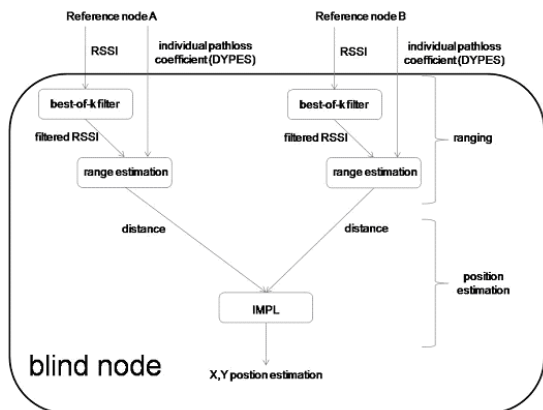


**Fig.14. Complete scheme for localization with two reference inputs**

We use the following parameters for all experiments if not explicitly stated different. The Improved REMA parameters are signal strength at 1m distance: A = 48dBm, number of past RSSI measurements for the best-of-k filter: k = 3, sample set size for localization is

set to 40 particles. The IMPL parameters (obtained heuristically) are measurement error mean: 1m, measurement error standard deviation: 20m, the maximum nodes speed is given as 2m/s plus an additional uncertainty factor of 1m. The localization and path loss updates are done each second. We refer to this system as a first version of our patient localization system (PLoc- V1).

**LOS Test Area**

We obtain a mean position estimation (localization) error of 13.93m. The average number of visible reference nodes during localization is around 6. It is observed that mean position estimation error is higher than the mean ranging error (12.21m, see table1). We believe this is due to the sensitivity of IMPL if fed with wrong ranging information. One wrong distance severely affects the position estimation of the system, whereas the mean ranging error is less affected by one wrong distance.

**NLOS Test Area**

In this experiment we test our localization system (PLoc-V1) in a realistic test area that reflects the attributes of a disaster site. The accuracy error plot is shown in figure 15. The blue dots show the number of visible nodes for each time step. For clarity reasons the number of visible nodes is multiplied by 10 to be shown in the same graph as the position error.

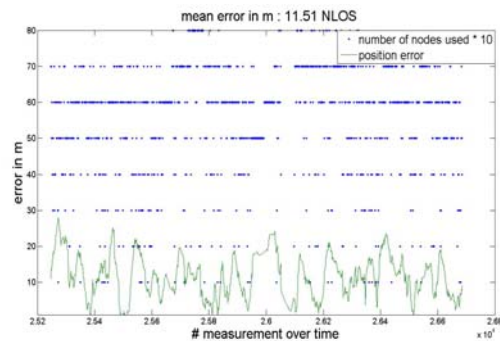


**Fig. 15. NLOS test area position estimation error**

The mean position error is 11.51m and the average number of visible reference nodes per time step is 5. The corresponding mean ranging error is 10.93 as in table 1. We can see that the accuracy is not severely affected by receiving less reference nodes inputs over certain time instances. The surface plot in figure 16 shows the mobility path of the blind node in NLOS test area and the corresponding position estimation error

(difference between actual position obtained from DGPS and the estimated position from PLoc) in different colours at each location of this mobility path. The surface plot plots locations with error less than approximately 20m in green colour.

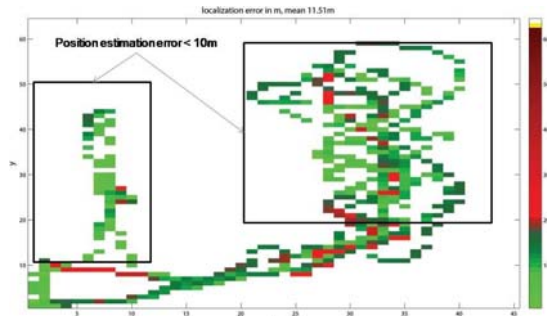


**Fig. 16. NLOS test area position estimation error- surface plot**

**PLoc-V1 Localization Results Summary**

Table 2 shows the localization results of Ploc-V1. We state that an average node visibility of 5 reference nodes per position estimation is sufficient for not affecting the position estimation accuracy significantly.

Test area	Area	RN	Mean error	Comment
LOS	80m×45m	8	13.93m	out-of-the-box
NLOS	60m×30m	8	11.51m	out-of-the-box

**Table 2. PLoc-v1 Localization performance**

**7 Comparison of PLoc-V1 and CC2431 Location System**

In this section the performance of PLoc-V1 is compared with the state-of-the-art localization system CC2431 from TI. The google image with reference node positions in figure 17 shows the experiment setup in a non line of sight environment with an area of 61 x 55m with 8 reference nodes deployed over the whole area. The area includes a parking lot, a walking pathway and has obstacles such as metal container, cars, fences and trees. We lowered the height of the reference nodes to 1m and placed a couple of nodes behind cars or other obstacles to simulate changing signal conditions. Compared to the test area used in the previous experiments (see figure 12) the non line of sight effect in this experiment area is larger and also includes additional lowering of the reference node height, to reflect adverse RF conditions. Two ZigBee

networks (one for PLoc-V1 and other for CC2431 system) operating in different channels are setup and a test person carrying the DGPS (actual position), the PLoc-V1 blind node and CC2431 blind node walks randomly in the test area with different speed and records the data. A static path loss coefficient has to be programmed upfront for the CC2431 system. It took around half an hour to select an optimized path loss coefficient (3.375) by testing the accuracy of this solution at different locations of the test area.

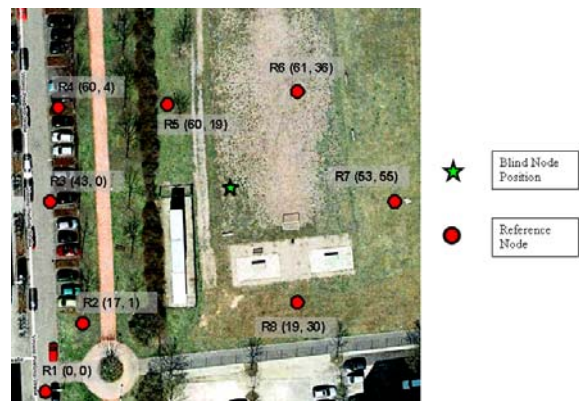


**Fig. 17. Test bed for comparison of PLoc-v1 and CC2431**

From the comparison of CC2431 and PLoc localization error in figure 18, it can be clearly seen that PLoc performs better in terms of average position error and outliers.

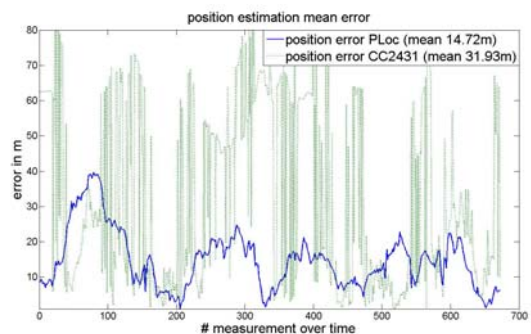


**Fig. 18. PLoc vs. CC2431 localization error**

It is observed in figure 18 that CC2431 error has frequent peaks with harsh error values which corrupt the range estimation. On the contrary PLoc error peaks are of lower values. This shows that CC2431 does not adapt to environmental changes leading to high distance variances. The localization error results are summarized as shown in table 3.

System	Path loss	Area(m)	Mean error
CC2431	3.375	61×55	31.93m
PLoc	Dynamic	61×55	14.72m

**Table 3. PLoc-v1 vs. CC2431 Localization performance**

The mean localization error for PLoc-v1 is higher in these experiments compared to the NLOS experiment mentioned in table2 due to the larger test area and lowering the reference node height which introduces additional signal fluctuations. The mean localization error of PLoc-v1 is 53% better than that of CC2431.

## 8. Conclusion and Future Works

In this paper a new algorithm called Ranging using Environment and Mobility Adaptive RSSI (REMA) is proposed. From the ranging experimentations in indoor and outdoor environments, we found that RSSI based ranging is a feasible solution for the localization in our scenario. With our proposed REMA, we are able to reduce the overall average range estimation error by about 31% when compared to that of the state of the art 'CC2431-Ranging'. This REMA acts as a suitable base and is further improved to propose the Improved REMA method for range estimation during patient localization at the disaster site.

A new RSSI based localization system (first release of PLoc-V1) is evaluated using a demonstrator. The mean localization error of PLoc-v1 that uses Improved REMA (best-of-k and DYPES) for ranging and IMPL for position estimation in a realistic test bed that reflects the attributes of a disaster site is 11-14m, which is closer to the accuracy specification for patient localization. Comparing the performance of PLoc-v1 with state of the art RSSI based localization system CC2431 in a realistic environment shows that the accuracy of PLoc is 53% better than the CC2431 system. Moreover, PLoc-v1 is an out-of-the-box system as it can dynamically calculate the path loss coefficient and adapt to environmental changes while CC2431 uses a static path loss and requires high installation time.

Further improvement of PLoc first release (ranging and position estimation techniques in terms of accuracy, scalability) for outdoor environment and testing of this system at indoor environment will be part of future work.

## 9. References

- [1] A. Chandra-Sekaran, P. Dheenathayalan, P. Weisser, C. Kunze, and W. Stork, "Empirical Analysis and Ranging using Environment and Mobility Adaptive RSSI Filter For Patient Localization during Disaster Management," in The 5th International Conference on Networking and Services (ICNS 2009), Valencia, Spain, 2009.
- [2] Chandra-Sekaran, A., et al., Efficient Resource Estimation During Mass Casualty Emergency Response Based on a Location Aware Disaster Aid Network, Heidelberg : Springer Berlin, European Conference on Wireless Sensor Networks Bologna Italy, vol. 4913/2008. ISSN0302-9743, 2008
- [3] ZigBee Specification, ZigBee Alliance Downloads, <http://www.zigbee.org>, ZigBee Alliance, 2008
- [4] CC2431 - System-on-Chip for 2.4 GHz ZigBee/ IEEE 802.15.4 with Location Engine, Data sheet, Texas Instruments
- [5] CC2430 - System-on-Chip for 2.4 GHz ZigBee/ IEEE 802.15.4, Data sheet, Texas Instruments
- [6] A. Baggio and K. Langendoen, "Monte Carlo localization for mobile wireless sensor networks," Ad Hoc Networks, vol. 6, pp. 718-733, 2008.
- [7] Kamin Whitehouse et. Al., Practical Evaluation of Radio Signal Strength for Ranging-based Localization.
- [8] Want, R., et al., The active badge location system, ACM Trans. Inf. Syst., pages 91-102, 1992
- [9] Priyantha, N. B., Chakraborty, A. and Balakrishnan, H., The Cricket Location Support System, ACM Press, Proceedings of the 6th annual international conference on Mobile computing and networking (MobiCom'00), pages 32-43, 2000
- [10] Bahl, P. and Padmanabhan, V., RADAR: An inbuilding RF based user location and tracking system, Proceedings of IEEE Infocom. vol. 2, pages 775-784, 2000
- [11] Global Positioning System <http://www.gps.gov/>
- [12] Erin-Ee-Lin Lau et. al., Enhanced RSSI-based Real-time User Location Tracking System for Indoor and Outdoor Environments.
- [13] Texas Instruments CC2431 Location Engine: Application Note AN042.
- [14] Christopher M. Bishop, Pattern recognition and machine learning
- [15] Shashank Tadakamadla, Indoor Local Positioning System For ZigBee, Based On RSSI, Mid Sweden University, the Department of Information Technology and Media (ITM), 2006
- [16] Muthukrishnan, Kavitha, Lijding, Maria and Havinga, Paul, Towards Smart Surroundings: Enabling Techniques and Technologies for Localization, Proceedings of the First International Workshop on Location- and Context-Awareness (LoCA), 2005
- [17] Masashi Sugano et. al., Indoor Localization System Using RSSI Measurement of WSN Based on ZIGBEE Standard
- [18] Dimitrios et. al., An Empirical Characterization of Radio Signal Strength Variability in 3-D IEEE 802.15.4 Networks Using Monopole Antennas

- [19] Emiliano Miluzzo et. al., Radio Characterization of 802.15.4 and Its Impact on the Design of Mobile Sensor Networks
- [20] Jeffrey Hightower and Gaetano Borriello. SpotON: An Indoor 3D Location Sensing Technology Based on RF Signal Strength
- [21] Tian He, Chengdu Huang. Range-Free Localization Schemes for Large Scale Sensor Networks
- [22] A. Chandra-Sekaran, P. Weisser, C. Kunze, and K. Mueller-Glaser, A Comparison of Bayesian Filter Based Approaches for Patient Localization During Emergency Response to Crisis, in *The Third International Conference on Sensor Technologies and Applications (SENSORCOMM 2009)*, Athens, Greece, 2009.
- [23] R. R. Rao and J. Eisenberg, Improving Disaster Management: The Role of IT in Mitigation, Preparedness, Response, and Recovery. National Academies Press, 2007.